ACS OMEGA

http://pubs.acs.org/journal/acsodf

Article

InP_3 Monolayer as a Promising 2D Sensing Material in SF_6 Insulation Devices

Xin Qin,* Chenchen Luo, Yaqian li, and Hao Cui

Cite This: *ACS Omega* 2021, 6, 29752−29758

Read Online

ACCESS | Metrics & More | Article Recommendations

ABSTRACT: In this letter, we perform a first-principles study on the adsorption performance of the InP_3 monolayer upon three SF_6 decomposed species, including SO_2, SOF_2, and SO_2F_2, to investigate its potential as a resistance-type, optical or field-effect transistor gas sensor. Results indicate that the InP_3 monolayer exhibits strong chemisorption upon SO_2 but weak physisorption upon SO_2F_2. The most admirable adsorption behavior is upon SOF_2, which provides a favorable sensing response (−19.4%) and recovery property (10.4 s) at room temperature as a resistance-type gas sensor. A high response of 180.7% upon SO_2 and a poor one of −1.9% upon SO_2F_2 are also identified, which reveals the feasibility of the InP_3 monolayer as a resistance-type sensor for SO_2 detection with recycle use via a heating technique to clean the surface. Moreover, the InP_3 monolayer is a promising optical sensor for SO_2 detection due to the obvious changes in adsorption peaks within the range of ultraviolet and is a desirable field-effect transistor sensor for selective and sensitive detection of SO_2 and SOF_2 given the evident changes of Q_T and E_g under the applied electric field.

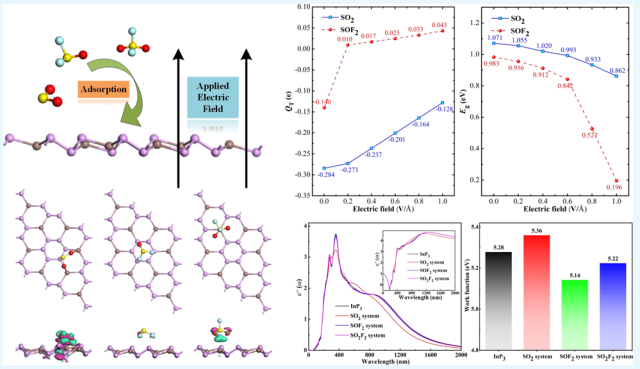

1. INTRODUCTION

Two-dimensional (2D) materials, such as graphene,[1] phosphorene,[2] transition metal dichalcogenides,[3] tellurene,[4] and carbon nitrides,[5] raise tremendous interest in the field of gas sensing due to their unique electronic behaviors, large specific surface area, and strong chemical reactivity.[6,7] Although there are many reports about 2D gas sensors, the exploration of novel 2D semiconductors with high carrier mobility, good stability, and desirable sensitivity upon some noble gases is still limited,[8,9] which in fact is highly desired in material and engineering fields. From this point of view, computationally predicting the potential of certain 2D nanomaterials for sensing application is a workable and high-effective manner of promoting the development of related fields.[10]

Very recently, a series of 2D metal phosphides including GeP_3,[11] CaP_3,[12] and InP_3[13] have been reported with high carrier mobility. In particular, the InP_3 monolayer is theoretically reported with high chemical stability, desirable indirect semiconducting property, and outstanding optical property,[14] which allows its application as a novel nanoelectronics. For example, Liu et al. reported the strong potential of the InP_3 monolayer to be explored as a reversible anode material for ultrafast charging.[15] Besides, the InP_3 monolayer has also been proposed as a sensing candidate for the detection of HCHO[16] based on the strain engineering, the n-type gas sensor for NO_2 sensing,[13] and sensing SF_6 decomposed species.[17] Therefore, the admirable electric performance of the InP_3 monolayer with a tunable band gap and good carrier mobility provides strong potential in the gas−surface interactions for further exploration of a novel 2D semiconductor.

SF_6 is widely used insulation medium in high-voltage devices to guarantee the safe operation of the power system.[18] However, in a long-running device, inevitable insulation defects would cause partial discharge and ionize SF_6, generating the F atom and low-fluorine sulfides. In most cases, these byproducts will recombine to SF_6, but in the presence of trace water and oxygen, they will continue to interact with these impurities and form several stable gas compounds such as SO_2, SOF_2, and SO_2F_2.[19] These noxious species would largely deteriorate the insulation behavior of SF_6, therefore threatening the safe operation of related devices. In this regard, the detection of SF_6 decomposed species using chemical gas sensors is proposed to evaluate the operation status of SF_6 insulation devices and ensure the safe running of the whole power system.[20,21]

Received: August 5, 2021
Accepted: October 13, 2021
Published: October 25, 2021

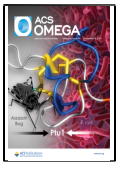

It has been investigated that the InP_3 monolayer has polar bonds that would form strong dipole−dipole forces with certain polar molecules.[16] Given the polar behavior of the SF_6 decomposed species, we assume that the InP_3 monolayer can exhibit strong interactions with the typical gas species. To verify our assumption, we in this letter theoretically investigate the adsorption and sensing behaviors of the InP_3 monolayer upon three SF_6 decomposed products (SO_2, SOF_2, and SO_2F_2) using first-principles theory. Our work means to explore the possible availability of the InP_3 monolayer as a sensing nanomaterial for detecting SF_6 decomposed species. In the meanwhile, most theoretical studies focus on exploring the resistance-type gas-sensing application of the InP_3 monolayer, while the optical and field-effect transistor sensing mechanisms of such 2D nanomaterials are less investigated. Thus, we will highlight such a perspective in this work to give detailed analysis about the InP_3-based gas sensor. It is our hope that the results in this work can stimulate further exploration of the InP_3 monolayer to be a resistance-type, optical or field-effect transistor gas sensor in the near future.

2. RESULTS AND DISCUSSION

The most energy-favorable configurations for SO_2, SOF_2, and SO_2F_2 adsorption onto the InP_3 monolayer were obtained by setting various initial adsorption structures with the initial distance of about 2 Å and selecting the one with the maximum E_{ad}. The gas molecules appear in different orientations to the possible adsorption sites of the InP_3 surface, including on the top of the P-hexatomic ring and the top of the In atom.

Figure 1 shows the most stable configurations and related electron density difference (EDD) for gas adsorptions, while Table 1 lists the adsorption parameters. From Figure 1, one can see that the SO_2 molecule prefers to be adsorbed on the top of a P atom with S being trapped, and two O atoms are trapped by the neighboring In atoms, whereas the SOF_2 and SO_2F_2 molecules tend to be trapped on the top of the P-hexatomic ring and the top of the In atom respectively, without the formation of new bonds. Then, newly formed P−S and In−O bonds are measured to be 2.36 and 2.30 Å, respectively. The shorter atomic distance between the InP_3 monolayer and the SO_2 molecule in comparison with that of SOF_2 (2.73 Å) and SO_2F_2 (3.51 Å) indicates the strong interaction in the former system. The calculated E_{ad} in the SO_2 system is −1.54 eV, exactly two times −0.77 eV in the SOF_2 system and about five times −0.31 eV in the SO_2F_2 system. These results manifest the strong chemisorption in the SO_2 system and favorable physisorption in the SOF_2 system; however, a quite weak interaction is identified in SO_2F_2 systems.[22] Such a finding, in our opinion, may attribute to the strong polar effect of the SO_2 molecule that can enhance the dipole−dipole force in the gas adsorption process. According to the Hirshfeld analysis, SO_2 and SOF_2 molecules are electron acceptors, receiving 0.28 and 0.12 e from the InP_3 monolayer, respectively, while the SO_2F_2 molecule is positively charged by only 0.05 e, suggesting its weak electron-donating behavior. These parameters consistently imply that the adsorption behavior of the InP_3 monolayer upon three gases is in the order SO_2 > SOF_2 > SO_2F_2. From EDD, the SO_2 molecule is surrounded by electron accumulation, and a dense electron overlap is seen on the P−S and In−O bonds, which suggests the orbital hybridization and illustrates the strong binding force between bonding atoms. On the contrary, such a phenomenon is unobvious in the SOF_2 and SO_2F_2 systems, indicating relatively weaker performance of the InP_3 monolayer upon their adsorptions.

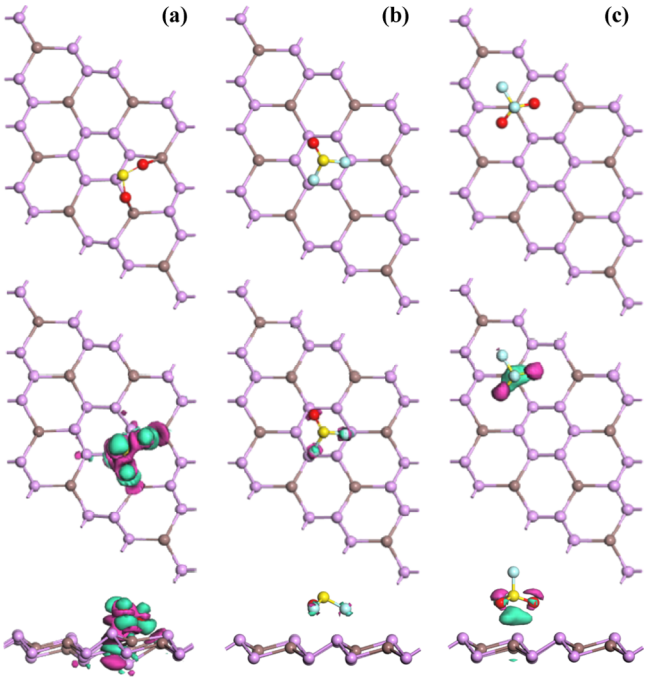

Figure 1. Most stable configurations and related EDD for (a) SO_2, (b) SOF_2, and (c) SO_2F_2 adsorption. In EDD, the cyan (rosy) areas are electron accumulation (depletion). The isosurface is 0.008 e/Å^3.

Table 1. Adsorption Parameters in Three Systems

systems	E_{ad} (eV)	Q_T (e)	D (Å)
SO_2	−1.54	−0.28	2.30
SOF_2	−0.77	−0.12	2.73
SO_2F_2	−0.31	0.05	3.51

Further analysis of the electronic behavior of the InP_3 monolayer upon gas adsorption is exhibited in Figure 2, in which the density of states (DOS) and total charge density (TCD) are plotted. From the total DOS, it is seen that the states around the Fermi level are somewhat deformed in the SO_2 system, especially at the top of the valence band and the bottom of the conduction band, while a little change is seen around the Fermi level in the SOF_2 and SO_2F_2 systems. Although remarkable deformations occur below −5.0 eV in three systems, we assume that these novel states at the deep valence band may not exert a really remarkable impact on the electronic behavior of the whole system.[23] In fact, the deformations of the total DOS attribute to the contribution from the activated DOS of adsorbed gas molecules. After adsorption, the DOS of SO_2 splits into several small peaks standing around the Fermi level from −2.5 to 2.5 eV, which leads to the formation of the total DOS near the Fermi level and therefore causes a change in the electronic behavior largely. On the other hand, the DOS of SOF_2 and SO_2F_2 after adsorption is left-shifted by about 3.0 eV, exerting small contribution to the states around the Fermi level and thus leading to a slight change in the electronic property of the whole system accordingly. From the TCD, the electron accumulation could be found at SO_2 and SOF_2 molecules, while electron depletion at the SO_2F_2 molecule is identified.

https://doi.org/10.1021/acsomega.1c04185
ACS Omega 2021, 6, 29752−29758

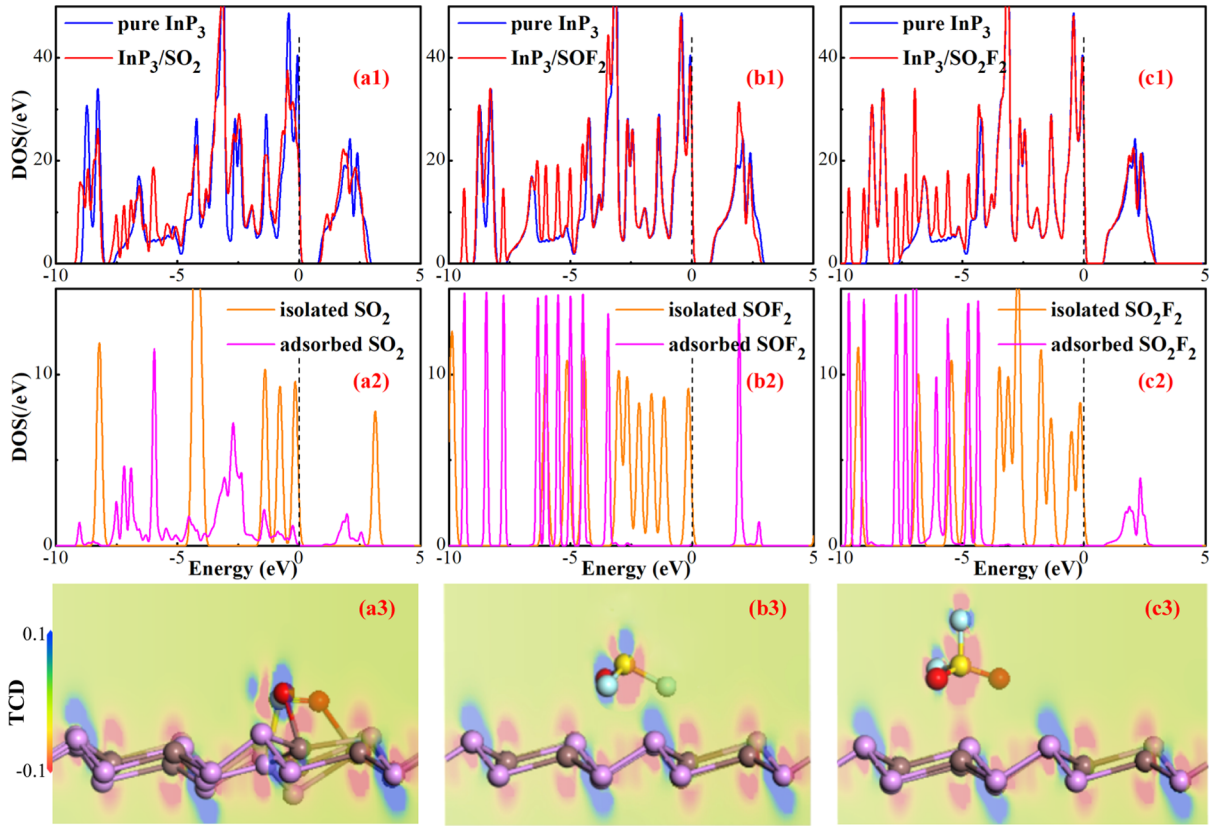

Figure 2. DOS and TCD of gas adsorption systems. The dash line is the Fermi level. (a1−a3) SO_2; (b1−b3) SOF_2; and (c1−c3) SO_2F_2.

These agree with the Hirshfeld analysis well. Also, the electron accumulation could be seen on the P−S and In−O bonds, confirming the strong orbital hybridization between these atoms.

The changed electronic behavior of the InP_3 monolayer ascribes to the adsorption of gas species, which results in the electron redistribution for the adsorbed systems,[13] and in this case, the band gap of the InP_3/gas system will differ from that of the pure InP_3 surface. According to our band structure calculations, the band gap of the primitive InP_3 monolayer is 1.018 eV, close to 1.14 eV reported previously.[16] Besides, the band gap of the SO_2 system rises to 1.071 eV, while that of SOF_2 and SO_2F_2 systems reduces to 0.983 and 1.017 eV, respectively. While the conductivity (σ) of materials is related to its band gap as $\sigma = \lambda\, e^{(-B_g/2kT)}$, wherein λ is a constant, B_g is the band gap, k is the Boltzmann constant, and T is temperature (set as 298 K in this work), the gas response (S) could be formulated as $S = (\sigma_{gas}^{-1} - \sigma_{pure}^{-1})/\sigma_{pure}^{-1}$, wherein σ_{gas} and σ_{pure}, respectively, mean the conductivity of the InP_3 monolayer after and before gas adsorption. Based on such two formulas, the responses for sensing SO_2, SOF_2, and SO_2F_2 molecules are calculated to be 180.7, −19.4, and −1.9%, respectively. In other words, the InP_3 monolayer could realize SO_2 detection with high sensitivity and exhibit a negative response upon SOF_2 and SOF_2F_2 sensing with a detectable response upon SOF_2 and limited response upon SO_2F_2. We should note that in the experimental research studies, there are some other parameters that can impact the electrical conductivity of the sensing materials, such as carrier mobility and surface decoration. However, in this work, we focus on the exploration of the pristine InP_3 monolayer as a sensing material; thus, the surface decoration manner is not mentioned, and if possible, some further research studies could be conducted to highlight such an important parameter. Besides, since the band gap is the most highlighted parameter to impact the electrical conductivity of the sensing materials applied in the theoretical research,[24] we herein use such a manner as well to evaluate the electrical conductivity of the InP_3 monolayer to analyze its sensing response in an easier and more effective manner.

The recovery time is another important parameter for estimating the ability for gas desorption from the sensor's surface, which is calculated by the van't Hoff−Arrhenius expression[25]

$$\tau = A^{-1}\, e^{(-E_a/K_B T)} \quad (1)$$

where A is the attempt frequency (10^{12} s^{-1}),[26] T is temperature, and K_B is the Boltzmann constant [8.318×10^{-3} kJ/(mol K)]. E_a is the potential barrier for gas desorption, which is assumed to be equal to E_{ad} here.[27,28] Equation 1 indicates that the larger the E_{ad}, the harder it is for gas desorption, and a higher temperature could help.

Figure 3 displays the recovery time of the InP_3 monolayer toward three gases at various temperatures. At ambient temperature (298 K), one can see that desorption for SO_2 is somewhat unrealistic and for SOF_2 is desirable, while the quite short time for SO_2F_2 desorption identifies its feeble interaction on the InP_3 surface. Via increasing the working temperature to 498 K, desorption of the stably adsorbed SO_2 from the InP_3 surface becomes feasible. Combining the sensing performance of the InP_3 monolayer, it could be inferred that the InP_3 surface is an admirable sensing material for SO_2 detection at room temperature, and its recycle use could be realized through heating at 498 K. Besides, the desirable sensing and

https://doi.org/10.1021/acsomega.1c04185
ACS Omega 2021, 6, 29752−29758

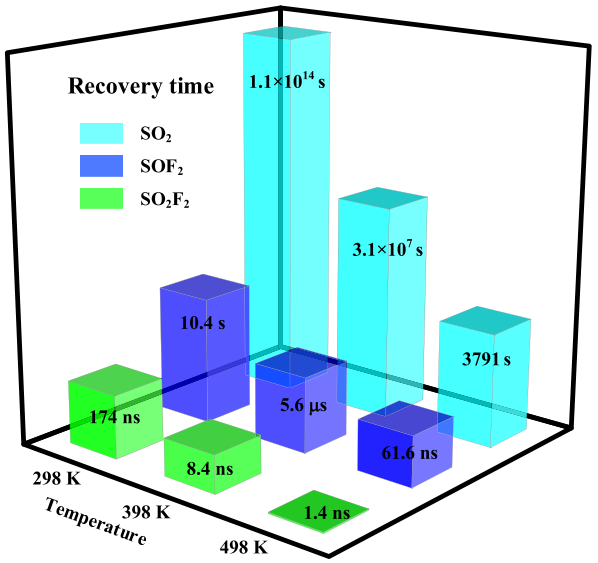

Figure 3. Recovery time of the InP_3 monolayer for gas desorption.

desorbing performances toward SOF_2 allow the application of the InP_3 monolayer as a reusable sensor under normal conditions. Moreover, such superior behavior of the InP_3 monolayer upon SO_2 and SOF_2 adsorption makes it applicable as a valid gas adsorbent to scavenge these noxious gases from SF_6 insulation devices, guaranteeing their safe operation effectively. However, the InP_3 monolayer is not suitable for SO_2F_2 sensing or removal due to the weak interaction in adsorption.

Figure 4 displays the dielectric functions and work function (WF) of the InP_3 monolayer upon gas adsorption. From Figure 4a, we can see two major adsorption peaks (277 and 356 nm) for the pure InP_3 surface, which within the range of ultraviolet is promising for gas detection due to its high energy.[29] After SO_2 adsorption, the peaks at 356 nm are remarkably weakened, and the peak at 277 nm suffers from a red shift to 285 nm. These findings suggest the sensitive detection of SO_2 using an InP_3 monolayer optical sensor. On the contrary, the slight change in adsorption intensity in SOF_2 and SO_2F_2 systems reveals the unfeasibility for their detection. From Figure 4b, one can see that the WF of the InP_3 monolayer suffers from a great increase after SO_2 adsorption and a more remarkable decrease after SOF_2 adsorption, while an unobvious decrease is determined in the SO_2F_2 system. The WF reveals the minimum energy required to release an electron from the surface, which impacts the performance of certain nanomaterials to be explored as a field-effect transistor gas sensor.[30] Based on these results, one can identify the potential of the InP_3 monolayer as a field-effect transistor sensor for sensitive and selective detection of SO_2 and SOF_2, given their obviously opposite changes of WF on the InP_3 surface.[31] However, both methods are not suitable for SO_2F_2 detection due to the weak response of the InP_3 monolayer upon gas adsorption.

In addition, the variations of Q_T and E_g in the SO_2 and SOF_2 systems tuned by the applied electric field are studied to further analyze the modulated sensitivity for their detection.[32] Such an electric field is vertical to the InP_3 surface pointing to the two gas species, with results shown in Figure 5. It is found that as the strength of the electric field increases from 0.2 to 1.0 V/Å, the Q_T is decreased in the SO_2 system but is increased in the SOF_2 system with the opposite charge-transferring path. In other words, the applied electric field can weaken the charge transfer from the InP_3 monolayer to the SO_2 molecule, while it accelerates the charge transfer from the SOF_2 molecule to the InP_3 surface. Such results are in good accordance with the WF analysis, wherein the opposite change of WF accounts for the different path of charge transfer when the extra electric field is applied. Associating with the change of Q_T, the E_g decreases sharply in the SOF_2 system, while it is slightly decreased in the SO_2 system. These findings manifest the desirable gas-sensing response of the InP_3 monolayer for SO_2 and SOF_2 detection as a field-effect transistor gas sensor,[33] especially for SOF_2 when the applied electric field is higher than 0.6 V/Å.

Based on the abovementioned analysis, further experimental research studies should be conducted to further verify our results, which would be the following work of our group. It is worth noting that to prepare the InP_3-based gas sensor, the interaction between the InP_3 nanomaterial and the substrate is very significant.[34] The main impact parameters include the texture of the substrate, deposition temperature, and exposure time and humidity in the air,[35] which are significant to ensure that the sensing materials can be doped on the substrates with the best-sensing performance using a proper thermal treatment technique. We are hopeful that such a highlight is beneficial to

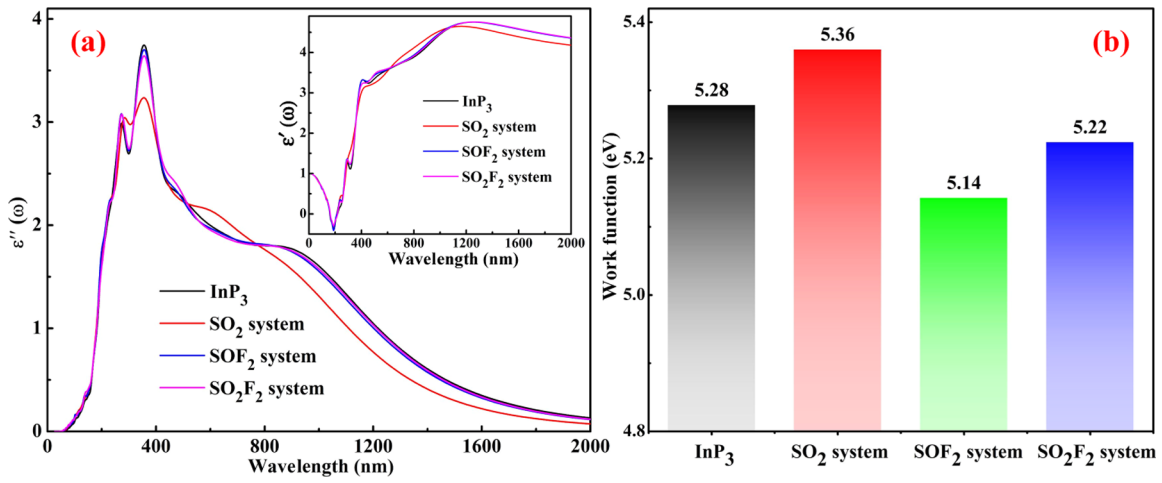

Figure 4. Dielectric functions (a) and WF (b) of the InP_3 monolayer upon gas adsorption.

https://doi.org/10.1021/acsomega.1c04185
ACS Omega 2021, 6, 29752−29758

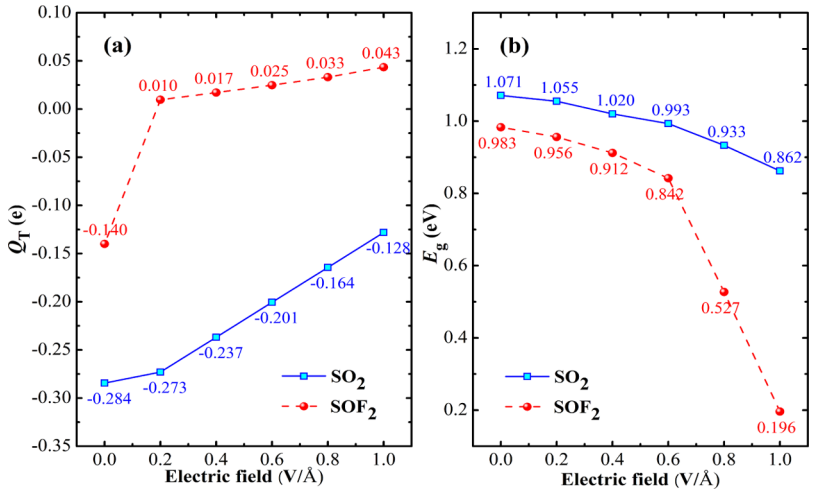

Figure 5. Variations of Q_T (a) and E_g (b) with the applied electric field.

help the experimental researchers to prepare an InP_3-based gas sensor with high gas sensitivity.

3. CONCLUSIONS

In this work, we provide a first insight into the InP_3 monolayer as a resistance-type, optical or field-effect transistor gas sensor upon three SF_6 decomposed species, namely, SO_2, SOF_2, and SO_2F_2, in order to evaluate the operation status of SF_6 insulation devices. The adsorption performances of the InP_3 monolayer upon three gases are in the order SO_2 > SOF_2 > SO_2F_2, in which strong chemisorption in the SO_2 system and weak physisorption in the SOF_2 system are identified. From the aspect of a resistance-type sensor, the InP_3 monolayer could realize sensitive detection of SO_2 with recycle use with the heating technique at 498 K. For SOF_2 sensing, the detectable response and desirable desorption property allow the working conditions of the InP_3 monolayer at room temperature. Moreover, the remarkable change in ultraviolet peaks of the InP_3 monolayer after adsorption of SO_2 indicates its optical sensing application, and the evident changes of WF of the InP_3 monolayer in two opposite trends illustrate the sensitive and selective detection between SO_2 and SOF_2. However, the InP_3 monolayer is not suitable for SO_2F_2 sensing due to the weak response in adsorption.

4. COMPUTATIONAL DETAILS

Spin-polarized calculations were implemented in this paper within the DMol^3 package.[36] The Perdew−Burke−Ernzerhof function within the generalized gradient approximation was employed to deal with the electron exchange−correlation terms.[37] The DFT-D2 method developed by Grimme was employed[38] to better understand the van der Waals force and long-range interactions. Double numerical plus polarization was selected as the atomic orbital basis set.[39] The Monkhorst−Pack k-point mesh of 12 × 12 × 1 was sampled for supercell calculations of geometric optimization and electronic properties.[40] The energy tolerance accuracy, maximum force, and displacement were set as 10^{-5} Ha, 2 × 10^{-3} Ha/Å, and 5 × 10^{-3} Å, respectively.[41] For static electronic calculations, a self-consistent loop energy of 10^{-6} Ha, global orbital cutoff radius of 5.0 Å, and smearing of 0.005 Ha were used to ensure the accuracy of total energy.[42]

We established a 2 × 2 × 1 primitive InP_3 monolayer supercell with a vacuum region of 15 Å to prevent possible interactions between adjacent units.[43] The lattice constant of the fully optimized InP_3 monolayer was obtained as 7.535 Å, equal to the previous theoretical work,[44] and the frequency ranges from 80.48 to 962.55 cm^{-1}, indicating the good stability of the InP_3 structure. The adsorption energy (E_{ad}) is calculated by

$$E_{ad} = E_{InP_3/gas} - E_{InP_3} - E_{gas} \quad (2)$$

where $E_{InP_3/gas}$, E_{InP_3}, and E_{gas} represent the total energies of the gas-adsorbed system, pure InP_3 monolayer, and isolated gas molecule, respectively. Moreover, the Hirshfeld method was considered to analyze the charge transfer (Q_T) in the gas adsorption systems, wherein the positive values indicated the electron-losing property of the adsorbed gas species.

AUTHOR INFORMATION

Corresponding Author

Xin Qin − *Academics Working Station, Changsha Medical University, Changsha 410219, China; Hunan Key Laboratory of the Research and Development of Novel Pharmaceutical Preparations, Changsha Medical University, Changsha 410219, China;* orcid.org/0000-0001-6275-4738; Email: qinxin@cqu.edu.cn

Authors

Chenchen Luo − *Maintenance Branch of State Grid Zhejiang Electric Power Limited Liability Company, Hangzhou 311232, China*

Yaqian li − *Academics Working Station, Changsha Medical University, Changsha 410219, China*

Hao Cui − *State Key Laboratory of Power Transmission Equipment & System Security and New Technology, Chongqing University, Chongqing 400044, China; College of Artificial Intelligence, Southwest University, Chongqing 400715, China;* orcid.org/0000-0002-9410-6345

Complete contact information is available at: https://pubs.acs.org/10.1021/acsomega.1c04185

Notes

The authors declare no competing financial interest.

https://doi.org/10.1021/acsomega.1c04185
ACS Omega 2021, 6, 29752−29758

■ ACKNOWLEDGMENTS

This work was supported in part by the Natural Science Foundation of Chongqing (no. cstc2020jcyj-msxmX0500) and the Independent Innovation Special Project of Beibei Science and Technology Bureau, Chongqing (no. 2021-3).

■ REFERENCES

(1) Sun, P.; Wang, K.; Zhu, H. Recent Developments in Graphene-Based Membranes: Structure, Mass-Transport Mechanism and Potential Applications. *Adv. Mater.* **2016**, *28*, 2287−2310.
(2) Bhimanapati, G. R.; Lin, Z.; Meunier, V.; Jung, Y.; Cha, J.; Das, S.; Xiao, D.; Son, Y.; Strano, M. S.; Cooper, V. R.; Liang, L.; Louie, S. G.; Ringe, E.; Zhou, W.; Kim, S. S.; Naik, R. R.; Sumpter, B. G.; Terrones, H.; Xia, F.; Wang, Y.; Zhu, J.; Akinwande, D.; Alem, N.; Schuller, J. A.; Schaak, R. E.; Terrones, M.; Robinson, J. A. Recent Advances in Two-Dimensional Materials beyond Graphene. *Acs Nano* **2015**, *9*, 11509−11539.
(3) Cui, H.; Jia, P.; Peng, X.; Li, P. Adsorption and sensing of CO and C2H2 by S-defected SnS2 monolayer for DGA in transformer oil: A DFT study. *Mater. Chem. Phys.* **2020**, *249*, 123006.
(4) Wang, D.; Yang, A.; Lan, T.; Fan, C.; Pan, J.; Liu, Z.; Chu, J.; Yuan, H.; Wang, X.; Rong, M.; Koratkar, N. Tellurene based chemical sensor. *J. Mater. Chem. A* **2019**, *7*, 26326−26333.
(5) Cui, H.; Yan, C.; Jia, P.; Cao, W. Adsorption and sensing behaviors of SF6 decomposed species on Ni-doped C3N monolayer: A first-principles study. *Appl. Surf. Sci.* **2020**, *512*, 145759.
(6) Feng, Z.; Xie, Y.; Chen, J.; Yu, Y.; Zheng, S.; Zhang, R.; Li, Q.; Chen, X.; Sun, C.; Zhang, H.; Pang, W.; Liu, J.; Zhang, D. Highly sensitive MoTe2 chemical sensor with fast recovery rate through gate biasing. *2D Materials* **2017**, *4*, 025018.
(7) Choi, S.-J.; Kim, I.-D. Recent Developments in 2D Nanomaterials for Chemiresistive-Type Gas Sensors. *Electron. Mater. Lett.* **2018**, *14*, 221−260.
(8) Cui, H.; Zhang, G.; Zhang, X.; Tang, J. Rh-doped MoSe2 as toxic gas scavenger: A first-principles study. *Nanoscale Adv.* **2019**, *1*, 772−780.
(9) Tongay, S.; Zhou, J.; Ataca, C.; Lo, K.; Matthews, T. S.; Li, J.; Grossman, J. C.; Wu, J. Thermally driven crossover from indirect toward direct bandgap in 2D semiconductors: MoSe2 versus MoS2. *Nano Lett.* **2012**, *12*, 5576−5580.
(10) Patel, K.; Roondhe, B.; Dabhi, S. D.; Jha, P. K. A new flatland buddy as toxic gas scavenger: A first principles study. *J. Hazard. Mater.* **2018**, *351*, 337−345.
(11) Jing, Y.; Ma, Y.; Li, Y.; Heine, T. GeP3: A small indirect band gap 2D crystal with high carrier mobility and strong interlayer quantum confinement. *Nano Lett.* **2017**, *17*, 1833−1838.
(12) Lu, N.; Zhuo, Z.; Guo, H.; Wu, P.; Fa, W.; Wu, X.; Zeng, X. C. CaP3: a new two-dimensional functional material with desirable band gap and ultrahigh carrier mobility. *J. Phys. Chem. Lett.* **2018**, *9*, 1728−1733.
(13) Yi, W.; Chen, X.; Wang, Z.; Ding, Y.; Yang, B.; Liu, X. A novel two-dimensional δ-InP3 monolayer with high stability, tunable bandgap, high carrier mobility, and gas sensing of NO2. *J. Mater. Chem. C* **2019**, *7*, 7352−7359.
(14) Miao, N.; Xu, B.; Bristowe, N. C.; Zhou, J.; Sun, Z. Tunable magnetism and extraordinary sunlight absorbance in indium triphosphide monolayer. *J. Am. Chem. Soc.* **2017**, *139*, 11125−11131.
(15) Liu, J.; Liu, C.-S.; Ye, X.-J.; Yan, X.-H. Monolayer InP3 as a reversible anode material for ultrafast charging lithium- and sodium-ion batteries: a theoretical study. *J. Mater. Chem. A* **2018**, *6*, 3634−3641.
(16) Yang, H.; Wang, Z.; Ye, H.; Zhang, K.; Chen, X.; Zhang, G. Promoting sensitivity and selectivity of HCHO sensor based on strained InP3 monolayer: A DFT study. *Appl. Surf. Sci.* **2018**, *459*, 554−561.
(17) Liao, Y.; Zhou, Q.; Peng, R.; Zeng, W. Adsorption properties of InP3 monolayer toward SF6 decomposed gases: A DFT study. *Phys. E* **2021**, *130*, 114689.
(18) Paul, T. A.; Kramer, A. Monitoring of SF6 Gas Admixtures in Gas-Insulated Electrical Equipment. *International Conference on Condition Monitoring and Diagnosis*, 2013; pp 493−496.
(19) Cui, H.; Liu, T.; Zhang, Y.; Zhang, X. Ru-InN Monolayer as a Gas Scavenger to Guard the Operation Status of SF6 Insulation Devices: A First-Principles Theory. *IEEE Sens. J.* **2019**, *19*, 5249−5255.
(20) Zhang, X.; Yu, L.; Tie, J.; Dong, X. Gas Sensitivity and Sensing Mechanism Studies on Au-Doped TiO2 Nanotube Arrays for Detecting SF6 Decomposed Components. *Sensors* **2014**, *14*, 19517−19532.
(21) Cui, H.; Zhang, X.; Zhang, J.; Zhang, Y. Nanomaterials-based gas sensors of SF6 decomposed species for evaluating the operation status of high-voltage insulation devices. *High Voltage* **2019**, *4*, 242−258.
(22) Allian, A. D.; Takanabe, K.; Fujdala, K. L.; Hao, X.; Truex, T. J.; Cai, J.; Buda, C.; Neurock, M.; Iglesia, E. Chemisorption of CO and mechanism of CO oxidation on supported platinum nanoclusters. *J. Am. Chem. Soc.* **2011**, *133*, 4498.
(23) Ma, D.; Wang, Q.; Li, T.; He, C.; Ma, B.; Tang, Y.; Lu, Z.; Yang, Z. Repairing sulfur vacancies in the MoS2 monolayer by using CO, NO and NO2 molecules. *J. Mater. Chem. C* **2016**, *4*, 7093−7101.
(24) He, X.; Gui, Y.; Xie, J.; Liu, X.; Wang, Q.; Tang, C. A DFT study of dissolved gas (C2H2, H2, CH4) detection in oil on CuO-modified BNNT. *Appl. Surf. Sci.* **2020**, *500*, 144030.
(25) Zhang, Y.-H.; Chen, Y.-B.; Zhou, K.-G.; Liu, C.-H.; Zeng, J.; Zhang, H.-L.; Peng, Y. Improving gas sensing properties of graphene by introducing dopants and defects: a first-principles study. *Nanotechnology* **2009**, *20*, 185504.
(26) Peng, S.; Cho, K.; Qi, P.; Dai, H. Ab initio study of CNT NO2 gas sensor. *Chem. Phys. Lett.* **2004**, *387*, 271−276.
(27) Chen, D.; Zhang, X.; Tang, J.; Cui, Z.; Cui, H. Pristine and Cu decorated hexagonal InN monolayer, a promising candidate to detect and scavenge SF6 decompositions based on first-principle study. *J. Hazard. Mater.* **2019**, *363*, 346−357.
(28) Wan, Q.; Chen, X.; Gui, Y. First-Principles Insight into a Ru-Doped SnS2 Monolayer as a Promising Biosensor for Exhale Gas Analysis. *ACS Omega* **2020**, *5*, 8919−8926.
(29) Peng, L.; Zhao, Q.; Wang, D.; Zhai, J.; Wang, P.; Pang, S.; Xie, T. Ultraviolet-assisted gas sensing: A potential formaldehyde detection approach at room temperature based on zinc oxide nanorods. *Sens. Actuators, B* **2009**, *136*, 80−85.
(30) Yang, A.; Pan, J.; Wang, D.; Lan, T.; Liu, Z.; Yuan, H.; Chu, J.; Wang, X.; Rong, M. Tunable SO2-sensing performance of arsenene induced by Stone-Wales defects and external electric field. *Appl. Surf. Sci.* **2020**, *523*, 146403.
(31) Wang, D.-W.; Wang, X.-H.; Yang, A.-J.; Chu, J.-F.; Lv, P.-L.; Liu, Y.; Rong, M.-Z. MoTe2: A Promising Candidate for SF6 Decomposition Gas Sensors with High Sensitivity and Selectivity. *IEEE Electron Device Lett.* **2018**, *39*, 292−295.
(32) Yang, A.; Wang, D.; Lan, T.; Chu, J.; Li, W.; Pan, J.; Liu, Z.; Wang, X.; Rong, M. Physics, Single ultrathin WO3 nanowire as a superior gas sensor for SO2 and H2S: Selective adsorption and distinct IV response. *Mater. Chem. Phys.* **2020**, *240*, 122165.
(33) Li, P.; Hong, Q.; Wu, T.; Cui, H. SOF2 sensing by Rh-doped PtS2 monolayer for early diagnosis of partial discharge in the SF6 insulation device. *Mol. Phys.* **2021**, *119*, No. e1919774.
(34) Giannazzo, F.; Sonde, S.; Nigro, R. L.; Rimini, E.; Raineri, V. Mapping the Density of Scattering Centers Limiting the Electron Mean Free Path in Graphene. *Nano Lett.* **2011**, *11*, 4612−4618.
(35) Armano, A.; Buscarino, G.; Cannas, M.; Gelardi, F. M.; Giannazzo, F.; Schilirò, E.; Lo Nigro, R.; Agnello, S. Influence of oxide substrates on monolayer graphene doping process by thermal treatments in oxygen. *Carbon* **2019**, *149*, 546−555.
(36) Delley, B. From molecules to solids with the DMol3 approach. *J. Chem. Phys.* **2000**, *113*, 7756−7764.
(37) Cui, H.; Zhang, X.; Zhang, G.; Tang, J. Pd-doped MoS2 monolayer: A promising candidate for DGA in transformer oil based on DFT method. *Appl. Surf. Sci.* **2019**, *470*, 1035−1042.

https://doi.org/10.1021/acsomega.1c04185
ACS Omega 2021, 6, 29752−29758

(38) Tkatchenko, A.; DiStasio, S. R., Jr.; Head-Gordon, M.; Scheffler, M. Dispersion-corrected Møller-Plesset second-order perturbation theory. *J. Chem. Phys.* **2009**, *131*, 094106.
(39) Zhang, X.; Yu, L.; Wu, X.; Hu, W. Experimental Sensing and Density Functional Theory Study of H2S and SOF2 Adsorption on Au-Modified Graphene. *Adv. Sci.* **2015**, *2*, 1500101.
(40) Monkhorst, H. J.; Pack, J. D. Special points for Brillouin-zone integrations. *Phys. Rev. B: Solid State* **1976**, *13*, 5188−5192.
(41) Cui, H.; Chen, D.; Zhang, Y.; Zhang, X. Dissolved gas analysis in transformer oil using Pd catalyst decorated MoSe2 monolayer: A first-principles theory. *Sustainable Mater. Technol.* **2019**, *20*, No. e00094.
(42) Ju, W.; Li, T.; Su, X.; Li, H.; Li, X.; Ma, D. Au cluster adsorption on perfect and defective MoS2 monolayers: structural and electronic properties. *Phys. Chem. Chem. Phys.* **2017**, *19*, 20735−20748.
(43) Wu, P.; Yin, N.; Li, P.; Cheng, W.; Huang, M. The adsorption and diffusion behavior of noble metal adatoms (Pd, Pt, Cu, Ag and Au) on a MoS2 monolayer: a first-principles study. *Phys. Chem. Chem. Phys.* **2017**, *19*, 20713−20722.
(44) Liu, J.; Liu, C.-S.; Ye, X.-J.; Yan, X.-H. Monolayer InP 3 as a reversible anode material for ultrafast charging lithium-and sodium-ion batteries: a theoretical study. *J. Mater. Chem. A* **2018**, *6*, 3634−3641.

https://doi.org/10.1021/acsomega.1c04185
ACS Omega 2021, 6, 29752−29758